Origin of the Cytochrome *a* Absorption Red Shift: A pH-Dependent Interaction between Its Heme *a* Formyl and Protein in Cytochrome Oxidase†

Patricia M. Callahan and Gerald T. Babcock*

ABSTRACT: Compared to low-spin heme *a* model compounds, the electronic absorption spectra of ferric and of ferrous cytochrome *a* are red shifted. Solvent effects are unable to account for the in vivo vs. in vitro differences; thus, a specific chromophore–protein interaction is likely. We have explored this possibility in detail by monitoring the alkaline pH dependence of the spectroscopic properties of oxidized and reduced cytochrome oxidase. Both heme *a* chromophores of the enzyme, cytochrome *a* and cytochrome a_3, undergo structural changes as the pH is increased, but by using several spectroscopic probes (optical absorption, MCD, EPR, and resonance Raman spectroscopies), we have been able to separate the pH dependencies of the two species. In both oxidation states, cytochrome a_3 is affected by alkaline pH in the range 8.5–10. The spectral shifts which occur are interpreted as arising from a high- to low-spin state change of the cytochrome a_3 heme iron and, for the reduced species, concurrent exposure of its normally hydrophobic pocket to the aqueous phase. Changes in the structure and environment of cytochrome *a* occur at higher pH (10–12). In the oxidized enzyme, cytochrome *a* shifts from its native, red-shifted, low-spin configuration to a five-coordinate high-spin species at pH 12 without forming discernible intermediate states. In the reduced enzyme, a Schiff's base is formed above pH 12. Prior to the formation of this species, the native structure of cytochrome *a* can be titrated ($pK_a \sim 10.5$) to produce an intermediate state with spectral properties characteristic of low-spin heme *a* model compounds in aqueous detergent solution. Over the same pH range the formyl vibration of cytochrome *a* relaxes from an abnormally low frequency (1610 cm^{-1}) to a frequency also characteristic of low-spin heme *a* models exposed to water (1633 cm^{-1}). We interpret these data to indicate that the absorption red shift of cytochrome *a*, its anomalous C=O stretching frequency, and its alkaline pH behavior result from a hydrogen-bonding interaction between its position 8 formyl group and a nearby amino acid residue, possibly the phenolic OH group of tyrosine. The hydrogen-bond strength apparently depends on the cytochrome *a* iron valence state, which suggests a mechanism by which redox-state changes at the heme are communicated to the protein.

Mitochondrial cytochrome oxidase consists of at least seven polypeptide subunits and four redox active metal centers, two heme *a* chromophores (**1**), and two copper ions, and catalyzes

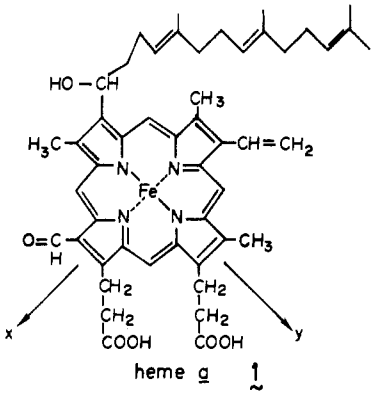

heme *a* (**1**)

the electron transfer reaction from cytochrome *c* to O_2. The metal centers act as electron transfer cofactors which apparently function in pairs; cytochrome *a* and Cu_a are the initial electron acceptors from cytochrome *c* and the second pair of metal ions, cytochrome a_3 and Cu_{a_3}, constitute the dioxygen reducing site [for reviews, see Malmström (1979), Wikström et al. (1981), and Babcock (1982)]. Cytochrome oxidase contributes to the buildup of the membrane free energy gradient during respiration both by consuming protons in the inner mitochondrial matrix during the dioxygen reduction reaction and by translocating protons across the inner mitochondrial membrane against the membrane electrochemical gradient (Wikström, 1977; Wikström & Saari, 1977). Subunit III may be involved in the development of this transmembrane proton gradient (Azzi, 1981), although recent observations on the two polypeptide *Paracoccus* cytochrome oxidase have rendered this interpretation somewhat ambiguous (Van Verseveld et al., 1981; Solioz et al., 1982); cytochrome *a* has been associated with the proton pumping action of the enzyme (Artzatbanov et al., 1978; Wikström & Krab, 1979), but the molecular mechanism remains to be elucidated.

The coordination geometries of cytochromes *a* and a_3 are well estabilished. Cytochrome *a* is six coordinate and low spin in both oxidation states (Tweedle et al., 1978; Blumberg & Peisach, 1979; Babcock et al., 1979a). Cytochrome a_3 is six coordinate and high spin ($S = {}^5/_2$) in the oxidized, resting enzyme (Babcock et al., 1981) and five coordinate and high spin ($S = 2$) in the reduced form (Babcock et al., 1976). It has recently been shown that cytochrome a_3 is in a hydrophobic environment as indicated by its Soret absorption maximum and formyl stretching frequency (Van Steelandt-Frentrup et al., 1981), as well as by the frequency position and line width of the C=O vibration in (carbon monoxy)cytochrome oxidase (Alben et al., 1981).

The longer wavelength absorbance maxima of cytochrome oxidase relative to protoheme-containing proteins results from its formyl-containing heme *a* chromophores (**1**). However, the individual contributions of cytochromes *a* and a_3 to the overall protein spectrum have been a source of considerable controversy in the past [for a review, see Malmström (1974)]. This has been resolved recently by evidence from several laboratories (Wikström et al., 1976; Wilson et al., 1978; Babcock & Salmeen, 1979; Scott & Gray, 1980; Halaka et al., 1981; Halaka, 1981; Babcock et al., 1981; Woodruff et

† From the Department of Chemistry, Michigan State University, East Lansing, Michigan 48824. *Received September 10, 1982.* This investigation was supported by the National Institutes of Health (GM 25480). P.M.C. is the recipient of a Monsanto Summer Fellowship. National Science Foundation Grant CHE-79-04810 to Michigan State University is acknowledged for the purchase of the EPR spectrometer.

0006-2960/83/0422-0452$01.50/0

Table I: Absorption Maxima and Formyl Stretching Frequencies of Cytochromes *a* and a_3 with Corresponding Heme *a* Model Compounds

heme *a* species	solvent	Soret (nm)	α (nm)	ν(C=O) (cm^{-1})
cytochrome a_3^{3+}		414[a]		1676[b]
(heme a^{3+})$(Me_2SO)_2$[c]	CH_2Cl_2	410		1672
cytochrome a_3^{2+}		443[a]		1665[d]
(heme a^{2+})(2-MeIm)[e]	CH_2Cl_2	442		1660
	H_2O	434		1640
cytochrome a^{3+}		425[a]	595	1650[g]
(heme a^{3+})$(NMeIm)_2$[c]	CH_2Cl_2	422	588	1670
	H_2O[h]	422	590	
cytochrome a^{2+}		444[a]	604	1610[g]
(heme a^{2+})$(NMeIm)_2$[e]	CH_2Cl_2	436[e]	588	1642
	H_2O	436[f]	594	1633[g]

[a] Vanneste (1966). [b] Ondrias & Babcock (1980). [c] Callahan & Babcock (1981). [d] Salmeen et al. (1978). [e] Van Steelandt-Frentrup et al. (1981). [f] Babcock et al. (1979b). [g] This work (see below). [h] Babcock et al. (1979a).

al., 1981) which support an independent chromophore model and indicate that the spectral deconvolution carried out by Vanneste (1966) provides reasonably accurate spectra of cytochromes *a* and a_3. By using the information described above on the coordination geometries of cytochromes *a* and a_3, it should be possible to prepare heme *a* model compounds which duplicate the optical properties of the in situ chromophores. The results of our recent efforts to accomplish this are summarized in Table I along with Vanneste's spectral data on cytochromes *a* and a_3. Heme *a* model compounds of the appropriate spin, coordination, oxidation state, and solvent environment reproduce well the spectral properties of the high-spin species, cytochrome a_3. Discrepancies arise, however, in the comparison of cytochrome *a* and low-spin heme *a*. The deconvoluted α band and Soret maxima of ferric and ferrous cytochrome *a* are considerably red-shifted relative to oxidized and reduced bis(*N*-methylimidazole)–heme *a*, which, by EPR[1] standards, is an appropriate cytochrome *a* model (Blumberg & Peisach, 1979; Babcock et al., 1979a). Moreover, the model compound spectra are only slightly sensitive to solvent, and thus, the unusual red shift of cytochrome *a*, which was originally noted by Lemberg (1962), may involve a fairly complex chromophore–protein interaction.

A second anomalous spectral characteristic of cytochrome *a* is apparent when the vibrational properties of its peripheral formyl group are compared with those of cytochrome a_3 and their respective model compounds (Babcock & Salmeen 1979; Babcock et al., 1981). For high-spin cytochrome a_3, the same heme *a* models which reproduce the optical properties also mimic the formyl stretching frequency (Table I), thus indicating that the position 8 aldehyde is free in a hydrophobic environment (Van Steelandt-Frentrup et al., 1981). On the other hand, the characteristic formyl vibration stretching frequencies observed for low-spin ferric and ferrous heme *a* model compounds are not apparent in the resonance Raman spectra of the enzyme (Table I).

Thus, the Raman data suggest a protein-induced alteration of the heme *a* formyl group in the cytochrome *a* binding site which, in turn, may be linked to the absorption red shift commented upon above. Such protein–chromophore interactions have been shown to be responsible for in vivo vs. in vitro spectral differences in other protein systems. For example, both the absorption red shift and vibrational properties of retinal in rhodopsin and bacteriorhodopsin have been accounted for to first order by the presence of a protonated Schiff base linkage between a lysine residue of the protein and the retinal aldehyde (Aton et al., 1977; Mathies et al., 1977; Marcus et al., 1979). Point charges in the vicinity of the chromophore have been advanced to explain further spectral differences (Honig et al., 1979; Sheves et al., 1979). Similarly, in photosynthetic systems, shifts in chlorophyll absorption spectra relative to those of model compounds have been attributed, in part, to perturbations induced by the protein environment (Davis et al., 1981). Finally, spectral differences between various formylated hemes when incorporated into apomyoglobin have been attributed to differences in local protein environments (Tsubaki et al., 1980).

Insight into such a protein–chromophore interaction in cytochrome oxidase can be obtained from data reported by Lemberg (1964) which showed that upon alkalinization of cytochrome oxidase solutions the spectrum of the reduced enzyme shifts to shorter wavelength in two distinct steps. In the first, the absorption maxima move to (Soret, α) 436 nm, 596 nm followed by a further blue shift to 428 nm, 575 nm. The latter species is clearly established as the Schiff base adduct of the heme *a* aldehyde which is stable at pH levels greater than 12 (Lemberg, 1964; Takemori & King, 1965). The basis of the initial absorption spectral shift to yield Soret and α maxima typical of low-spin ferrous heme *a* in an aqueous environment was attributed to an unspecified conformational change of the protein. This work was extended in Soret excitation resonance Raman experiments by Salmeen et al. (1978), who observed several changes in vibrational frequencies as the pH was raised and noted that the species absorbing at 436 nm, 595 nm, formed at pH 11.5, gives rise to a spectrum that is similar to the resonance Raman spectrum of (heme a^{2+})$(Im)_2$ in aqueous detergent solution.

We have reinvestigated these pH induced effects on the optical properties of cytochrome oxidase by using resonance Raman, MCD, and EPR spectroscopies as probes to understand the anomalous spectral features of cytochrome *a*. The magnetic techniques are useful in that changes in heme *a* spin state may be monitored. Resonance Raman spectroscopy provides similar information on coordination geometries through analysis of the structure sensitive vibrations of the porphyrin macrocycle (Callahan & Babcock, 1981). Moreover, Raman detection of the formyl stretching vibration provides additional insight into the chromophore because this mode is sensitive to solvent effects, covalent interactions, and hydrogen-bonding effects. By using this approach, we have been able to detect and assign the cytochrome *a* formyl stretching vibration. We interpret the combination of red-shifted absorption spectrum and altered formyl vibration as arising from a pH-dependent hydrogen-bonding interaction between a protein residue, possibly tyrosine, and the cytochrome *a* formyl group. A preliminary account of some of the research described here has been given elsewhere (Callahan & Babcock, 1982).

Materials and Methods

Beef heart cytochrome oxidase was isolated and its inhibitor complexes were prepared as described previously (Babcock et al., 1976; Babcock & Salmeen, 1979). The buffer–detergent system used for neutral and inhibitor complexes consisted of 0.5% lauryl maltoside–50 mM Hepes, pH 7.4; the buffer–

[1] Abbreviations: MCD, magnetic circular dichroism; EPR, electron paramagnetic resonance; RRS, resonance Raman spectroscopy; Hepes, *N*-(2-hydroxyethyl)piperazine-*N*′-2-ethanesulfonic acid; TMPD, *N*,*N*,*N*′,*N*′-tetramethyl-*p*-phenylenediamine; CHES, 2-(*N*-cyclohexylamino)-ethanesulfonic acid; CAPS, cyclohexylaminopropanesulfonic acid; $NaDodSO_4$, sodium dodecyl sulfate; NMeIm, *N*-methylimidazole; Im, imidazole; CTAB, cetyltrimethylammonium bromide.

detergent system used for the pH studies was 0.5% cholate–50 mM potassium phosphate buffer. The enzyme solutions were brought to the desired pH levels with 1 N NaOH and incubated for approximately 6 h at 4 °C. We found the slow kinetics of the pH-induced protein alteration to be a hindrance in these experiments in that the final states achieved may reflect both thermodynamic and kinetic effects. Lemberg (1964) has also commented upon this difficulty. Nonetheless, the effects we observe at high pH are reproducible and we have adopted an equilibrium viewpoint in discussing the phenomena. Reduction of the enzyme, which is slower at alkaline pH, was achieved by the addition of 20 mM ascorbate–0.2 mM TMPD. The pH-induced spectral shifts were also observed in other buffers and detergents, e.g., CHES, CAPS, glycine, lauryl maltoside, and Tween-20, although in the pH range 8–11.5 the spectral shifts were not as dramatic as for the cholate–phosphate system, in agreement with similar observations made previously (Lemberg & Pilger, 1964; Chan et al., 1970). The pH values reported are those measured immediately after the experiment was complete.

The chloride complex of heme *a* was isolated from purified beef heart cytochrome oxidase as described previously (Babcock et al., 1976). The ferrous high-spin species was prepared in aqueous solvent with 0.3 M 2-MeIm, 0.07 M CTAB, and 0.1 M potassium phosphate, pH 7.4, and reduced by addition of a few grains of solid dithionite (Virginia Smelting).

Raman spectra were recorded by using a Spex 1401 double monochromator and the associated Ramalog electronics. Soret excitation spectra were obtained with the 406.7- and 413.1-nm lines of a Spectra Physics 164-11 krypton ion laser equipped with high-field magnet. Power incident on the sample was typically 20–40 mW. Spectra of oxidized cytochrome oxidase were obtained with a flowing sample arrangement as previously reported (Babcock & Salmeen, 1979). All spectra were collected in 90° scattering geometry and enzyme samples were maintained chilled at 4 °C. Excitation in the 600-nm region was obtained from a Spectra Physics dye laser (Model 375) with Rhodamine 6G dye pumped by a Spectra Physics Model 165 argon ion laser. Power incident on the sample was typically 50–80 mW. Optical spectra were recorded before and after each spectroscopic experiment to monitor sample integrity by using either a Cary 17, a Cary 219, or a McPherson EU-707D recording spectrophotometer. EPR spectra were recorded by using a Bruker ER200D X-band spectrometer; operation at low temperature was achieved by using an Oxford ESR-9 liquid helium cryostat. MCD spectra taken at the University of Michigan were obtained with a JASCO J-40C recording spectropolarimeter equipped with a MCD-1 electromagnet operating at 16.05 kG, Data General Nova 3 minicomputer, and Tracor Northern PN-1500 digital signal analyzer. MCD spectra taken at the University of California, Berkeley, were recorded by using the computer-interfaced spectrophotometer described previously (Sutherland et al., 1974).

Results

Oxidized Cytochrome Oxidase pH Effects. For oxidized cytochrome oxidase, the pH dependence of the resonance Raman spectrum is shown in Figure 1 and of the visible absorption spectrum in Figure 2. At pH 7.4, the high-frequency vibrations of cytochrome a^{3+} occur at 1650, 1641, 1590, 1506, 1474, and 1373 cm^{-1} and those of cytochrome a_3^{3+} are observed at 1676, 1615, 1572, 1477, and 1373 cm^{-1} (Babcock et al., 1981). At pH 10 vibrational band shifts are observed as follows: (a) a decrease in intensity of the cytochrome a_3^{3+} 1572-cm^{-1} band, (b) increases in intensity at 1590 and 1641 cm^{-1}, and (c) a decrease in intensity and frequency shift in the a_3 formyl vibration from 1676 to 1673 cm^{-1}. The changes that occur in the optical absorption spectrum in this pH range (Figure 2) are (a) decreased absorbance at 655 nm, (b) increased absorbance at 600 nm, and (c) a red shift in the Soret

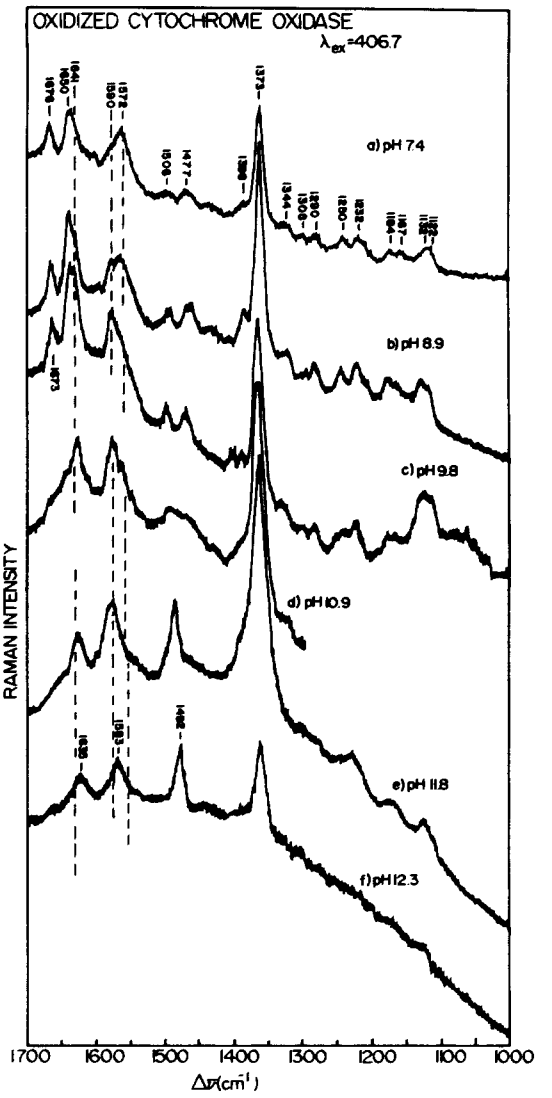

FIGURE 1: Resonance Raman spectra of oxidized cytochrome oxidase at several pH levels obtained with 406.7-nm excitation. Enzyme concentration was approximately 30–50 μM (heme *a* basis). Instrumental conditions: resolution, 6 cm^{-1}; time constant, 1 s; scan rate, 50 cm^{-1}/min.

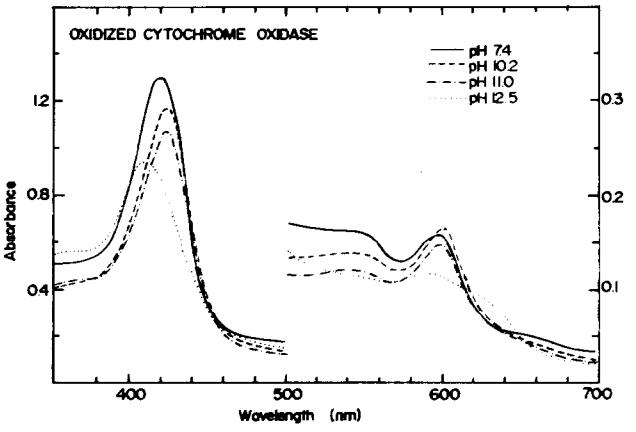

FIGURE 2: Optical absorption spectra of oxidized cytochrome oxidase at several alkaline pH levels. Enzyme concentration was approximately 10–15 μM (heme *a* basis) for all samples.

Table II: Absorption Maxima and Individual Chromophore Formyl Vibrational Assignments of Reduced Cytochrome Oxidase at Neutral and Alkaline pH

pH	Soret (nm)	α (nm)	$\nu(C=O)_{a_3}{}^{2+}$ (cm^{-1})	$\nu(C=O)_{a}{}^{2+}$ (cm^{-1})
7.4	443	604	1665	1610
9.5	441	601	1633	1610
11.5	436	596	1633	1633
12.5	428	575		

maximum from 420 to 425 nm. The apparent midpoint for this shift is ~9.5. These changes are consistent with a high- to low-spin transition of the cytochrome a_3 chromophore as the pH is increased. The core-size marker vibrations of a six-coordinate high-spin heme *a* model at 1572 and 1615 cm^{-1} disappear and are replaced by increased intensity in the corresponding modes of a six-coordinate, low-spin heme *a* species at 1590 and 1641 cm^{-1} (Callahan & Babcock, 1981). The shift in the cytochrome $a_3{}^{3+}$ formyl vibration from 1676 to 1673 cm^{-1} and the optical absorption spectral shifts are also indicative of increased low-spin character at alkaline pH (Callahan & Babcock, 1981; see below). EPR spectra of a similar series of enzyme samples (data not shown) taken under low-power (2 mW), low-temperature (10 K) conditions show a low-spin heme absorption in the pH range 8.5–10.8 with *g* values of 2.58, 2.3, and 1.80, indicative of the low-spin hydroxide form of heme a^{3+} (Wever et al., 1977). The spin concentration represented by this signal increases with increasing pH up to 10 and subsequently decreases as the pH is increased further. Even at maximum intensity, however, it represents considerably less than one heme per cytochrome oxidase. Similar behavior in the EPR spectrum was observed at moderately alkaline pH by Hartzell & Beinert (1974). No observable changes in the Raman intensity of the anomalous cytochrome a^{3+} vibration at 1650 cm^{-1} occur in this pH range; only under strongly denaturing conditions is this vibration affected.

At very high pH (~12), the Soret is broadened and blue-shifted to 413 nm. The visible region shows no distinct maxima although there is an increased absorbance at 635 nm. The major vibrational frequencies observed at pH 12 for the oxidized enzyme are 1635, 1583, 1492, and 1373 cm^{-1}. These band positions are similar to those observed for five-coordinate, high-spin heme a^{3+} (Callahan & Babcock, 1981). Electron paramagnetic resonance (EPR) spectra of alkaline pH enzyme samples result in a gradual decrease and disappearance in the low-spin cytochrome a^{3+} resonance at $g = 3$, with an apparent p*K* in the range 10–10.5, in agreement with the RR observations which show the absence of any low-spin species at pH 12. Although the Raman and optical absorption spectra at pH 12 suggest five-coordinate high-spin heme a^{3+} species, no high-spin EPR signal is observed at alkaline pH. This suggests severe protein denaturation in this pH range with release and subsequent aggregate, possibly μ-oxo dimer, formation by the free heme *a* chromophores. Supporting evidence for this configuration of the heme *a* chromophores lies in the similarity of the optical absorption properties of oxidized cytochrome oxidase at pH 12 and the previously reported data for heme *a* μ-oxo dimers (Caughey et al., 1975).

Reduced Enzyme pH Effects. Reduced cytochrome oxidase also shows a series of absorption shifts as the pH of the medium is raised (Figure 3). The Soret and α maxima gradually shift from (Soret, α) 443 nm, 604 nm at pH 7.4 to 436 nm, 598 nm at pH 11.0 (Table II). In the Soret region, cytochromes *a* and a_3 make roughly equal contributions to the absorption spectrum at neutral pH (Vanneste, 1966). In the α-band region, however, cytochrome a^{2+} is the dominant absorber. Thus, the shift of the oxidase α maximum from 604 to 596 nm as the pH of the reduced enzyme is raised implies that cytochrome *a* is being perturbed, as noted originally by Lemberg & Pilger (1964). The pH dependence of the half-bandwidth at half-height of the visible absorption band is shown in Figure 5. This titration curve has a p*K* of approximately 10.5. The half-bandwidths of ferrous low-spin heme *a* model compounds vary with solvent from approximately 300 cm^{-1} in nonpolar solvent to 500 cm^{-1} in an aqueous environment (Babcock et al., 1979b). Similarly, the two extremes of the titration curve correspond to half-bandwidths of approximately 300 and 500 cm^{-1} for the α band of cytochrome oxidase at neutral and alkaline pH. This observation suggests that a solvent environment change occurs at the low-spin heme chromophore, cytochrome a^{2+}, as the pH is increased. Because of the overlapping absorption spectra of the oxidase heme *a* chromophores and because we suspected alkaline modification of cytochrome $a_3{}^{2+}$ as well (Salmeen et al., 1978), we have used three other spectroscopic probes to identify more conclusively the shifts arising from the individual heme centers.

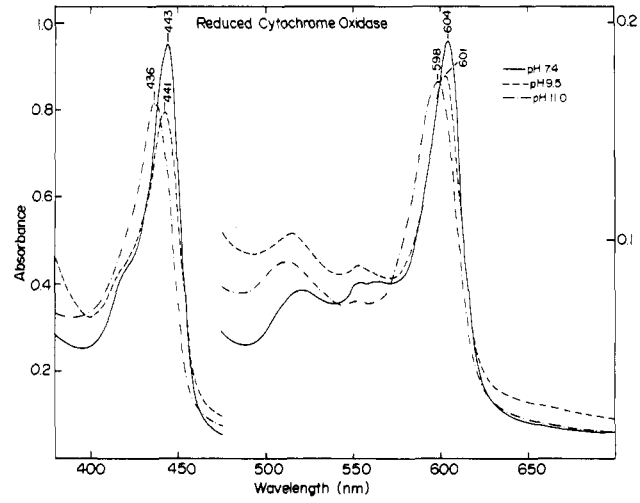

FIGURE 3: Optical absorption spectra of reduced cytochrome oxidase at several pH levels. Enzyme concentrations are approximately 6–8 μM.

The MCD spectrum of reduced cytochrome oxidase has distinct contributions from cytochromes a^{2+} and $a_3{}^{2+}$, thus offering a probe of the structural changes which occur at each of the individual chromophores at alkaline pH. An intense [$\Delta\epsilon/H$ = 79.3 $(M \cdot cm \cdot T)^{-1}$ at 446.7 nm] asymmetric A- and C-term MCD spectrum is observed for the native enzyme (Figure 4), which arises mainly from high-spin cytochrome $a_3{}^{2+}$ (Babcock et al., 1978). Spectra obtained for low-spin species, cytochrome a^{2+} and (heme a^{2+})$(NMeIm)_2$, are less intense [$\Delta\epsilon/H$ = 35.0 and 27 $(M \cdot cm \cdot T)^{-1}$ at 452 nm, respectively] and more symmetric (Babcock et al., 1979a). In addition to the MCD intensity differences, the various coordination and spin states of cytochromes a^{2+} and $a_3{}^{2+}$ and isolated heme *a* complexes have characteristic Soret region trough/peak ratios: cytochrome $a_3{}^{2+}$, 0.5; high-spin heme a^{2+} in ethylene glycol, 0.5; cytochrome a^{2+}, 0.75; low-spin (heme a^{2+})$(NMeIm)_2$, 1.0. These features can be used to monitor the properties of cytochromes *a* and a_3 as the pH is changed. Figure 4 reproduces MCD spectra of reduced cytochrome oxidase at neutral and at alkaline pH. The variation of the Soret MCD trough/peak ratio vs. pH is summarized for the reduced enzyme in Figure 5. The initial value of 0.5 increases gradually to a value of 0.7 in the pH range 9.5–10. This MCD ratio of 0.7 and the absorption spectrum of reduced cytochrome oxidase at pH 10 are similar to the spectral properties obtained

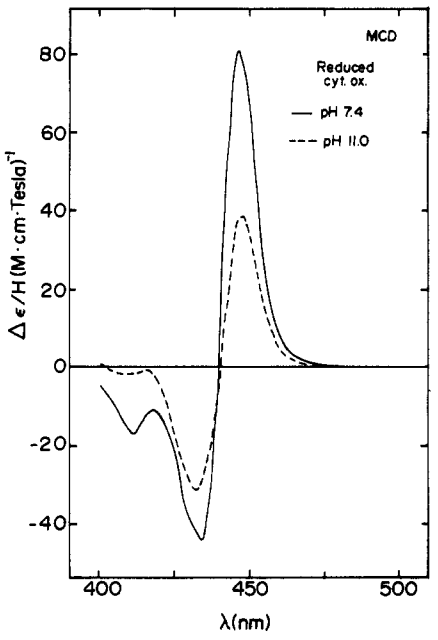

FIGURE 4: MCD spectra of reduced cytochrome oxidase at pH 7.4 and 11.0. Enzyme concentration is 10 μM.

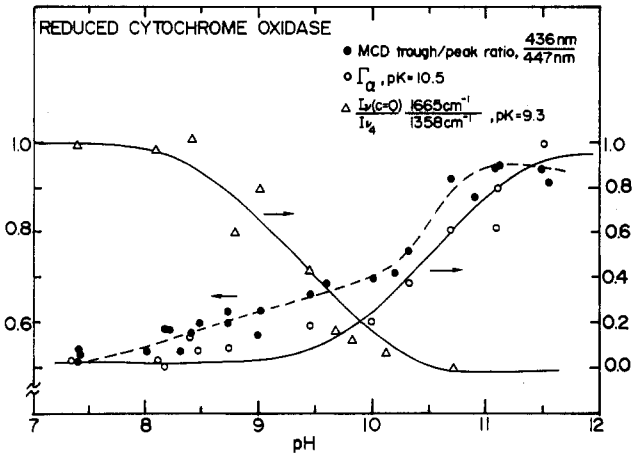

FIGURE 5: Titration curves as a function of pH for several spectral parameters of reduced cytochrome oxidase. Open circles are normalized α-band half-widths at half-height calculated from the formula $(\Gamma_\alpha)_{\text{normalized}} = [(\Gamma_\alpha)_{pH} - (\Gamma_\alpha)_{pH\,7.4}]/[(\Gamma_\alpha)_{pH\,11.5} - (\Gamma_\alpha)_{pH\,7.4}]$. The solid line is that calculated for pK = 10.5. Filled circles represent data points of MCD trough/peak (436 nm/446.7 nm) ratio. Open triangles represent the normalized intensity ratio of ν(C=O)/ν_4; the solid line is that calculated for pK = 9.3.

for the fully reduced enzyme plus cyanide (Babcock et al., 1976). The minor absorption band in the reduced enzyme optical spectrum at 565 nm, which is absent in inhibitor complexes that convert cytochrome a_3 to a low-spin species (HCN, CO), is also absent at pH 10 (Figure 3). These two pieces of data suggest that cytochrome a_3^{2+} undergoes a high- to low-spin transition in the pH range 8.5–10. The trough/peak ratio further increases to a value of 1.0 at pH 11.5. This pH-dependent step is responsible for the shift from a trough/peak ratio characteristic of cytochrome a^{2+} (0.7) to a ratio typical of a low-spin heme a^{2+} model compound (1.0). This final species also has absorption maxima corresponding to those of isolated low-spin heme a [(Soret, α) 436 nm, 596 nm, respectively]. Further increases in this MCD parameter at strongly alkaline pH (>12) can be attributed to Schiff base formation at the hemes a aldehydes as determined by the characteristic α-band absorption maximum of 575 nm. Attempts to calculate a titration curve of the MCD trough/peak

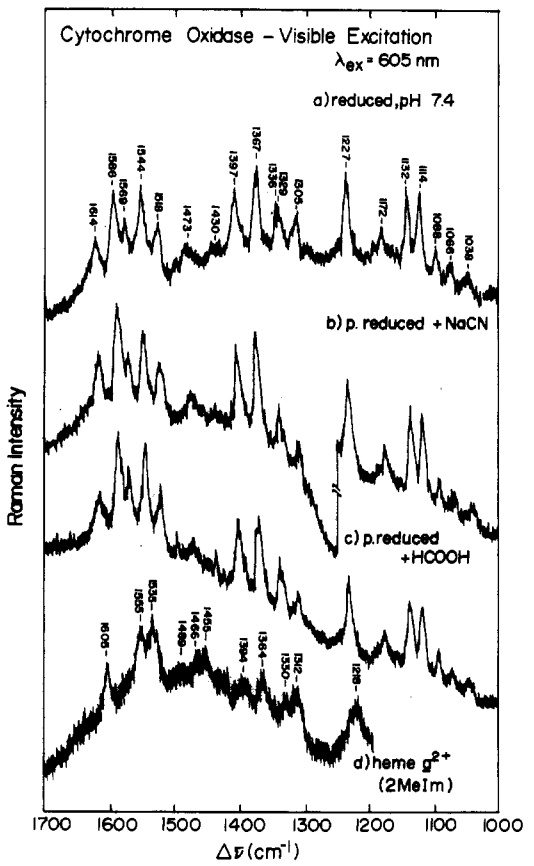

FIGURE 6: Visible excitation resonance Raman spectra of reduced cytochrome oxidase (a) and partially reduced inhibitor complexes (b and c). The spectrum in (c) was obtained with a flowing sample arrangement. Enzyme concentration was approximately 200 μM. The sample conditions in (d) are ~200 μM heme a–0.5 M 2-methylimidazole, in 0.07 M CTAB–0.1 M sodium phosphate–0.001 M EDTA, pH 7.4, with sodium dithionite as the reductant. Instrumental conditions: resolution, 5 cm^{-1}; for (a–c), time constant 1 s and scan rate 50 cm^{-1}/min; for (d), time constant 2.5 s and scan rate 20 cm^{-1}/min.

ratio from contributions of the individual chromophores were unsuccessful in mimicking the observed results. This may be a reflection of the heterogeneity of sites (Brudvig et al., 1981) or of the time dependence of the alkaline pH effects (Lemberg & Pilger, 1964).

Visible excitation resonance Raman spectroscopy provides a second probe and a more exact separation of the cytochromes a^{2+} and a_3^{2+} pH-dependent spectral shifts owing to the selective enhancement of the vibrations of one chromophore over the other. Figure 6 shows the resonance Raman spectra of reduced cytochrome oxidase and its partially reduced inhibitor complexes (Figure 6a–c) obtained with α-band excitation at 605 nm. The Raman spectra are similar regardless as to whether cytochrome a_3 is ferrous, five coordinate, and high spin (Figure 6a) or ferric, six coordinate, and low spin (Figure 6b) or high spin (Figure 6c) (Bocian et al., 1979). Because of the well-documented dependence of resonance Raman band position and intensity upon heme coordination geometry and extinction coefficient in the Herzberg–Teller scattering region (Spaulding et al., 1975; Spiro et al., 1979), we would expect these alterations in cytochrome a_3 spin and valence states to be reflected by shifts in the Raman spectrum if it were a strong absorber in the α-band region. However, the visible excitation resonance Raman spectra of Figure 6 are essentially identical, independent of the oxidation, coordination, or spin state of cytochrome a_3, and therefore we attribute the vibrations observed to cytochrome a^{2+} and make the corollary conclusion

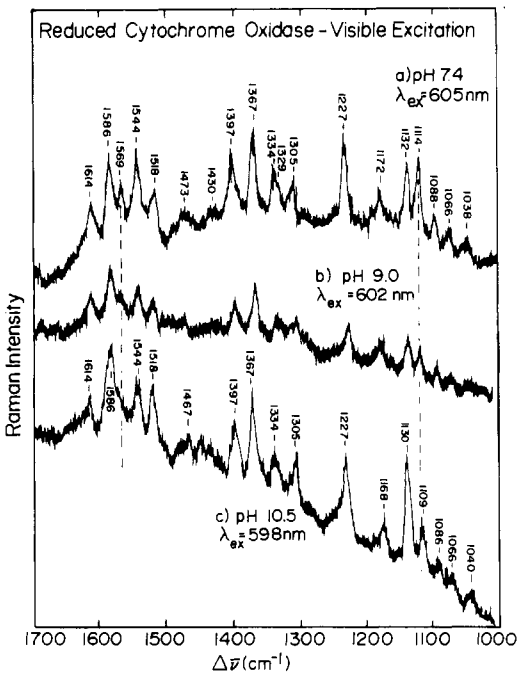

FIGURE 7: Visible excitation resonance Raman spectra of reduced cytochrome oxidase at several pH levels, with excitation wavelength as noted in the figure. Enzyme concentration was 200–300 μM (heme *a* basis). Instrumental conditions: resolution, 5 cm^{-1}; time constant, 2.5 s; scan rate, 20 cm^{-1}/min.

that it is the dominant absorber in this region. Furthermore, the prominent vibrations of (heme a^{2+})(2-MeIm) (Figure 6d) at 1533, 1555, and 1605 cm^{-1}, a model for the coordination and spin state of cytochrome $a_3{}^{2+}$ (Van Steelandt-Frentrup et al., 1981), are not observed in the RR spectra of reduced cytochrome oxidase, thereby providing additional evidence that vibrations of cytochrome a^{2+} alone are observed under these conditions. Visible excitation Raman spectra, then, can be used to monitor the pH dependence of a single heme chromophore, cytochrome a^{2+}. Resonance Raman spectra obtained with visible excitation of reduced cytochrome oxidase at several alkaline pH levels are shown in Figure 7. The changes observed are (a) a reduction in intensity of the 1569- and 1329-cm^{-1} bands and (b) a decrease in intensity and shift in frequency of the 1114-cm^{-1} vibration to 1109 cm^{-1}. These pH effects titrate over the pH 10–11.5 range. Since the vibrations observed with visible excitation of the reduced enzyme at neutral pH arise solely from cytochrome a^{2+} and noting the fact that no new vibrations are observed with visible excitation at alkaline pH, this suggests that the spectral shifts occurring with a pK ~ 10.5 arise from a pH-dependent modification of cytochrome a^{2+}.

For documentation of the pH dependencies of the two heme centers further, Soret excitation resonance Raman spectroscopy has been employed as a third technique. The selective enhancement of the vibrations of a single chromophore by proper choice of excitation frequency for the partially reduced inhibitor complexes of cytochrome oxidase is not feasible at alkaline pH because of the unfavorable pK values of HCN and HCOOH. For this reason, we are limited to the pH study of the fully reduced enzyme. Although complicated by the fact that vibrations of both chromophores are enhanced, Soret excitation resonance Raman spectra can yield significant structural information. The Soret resonance Raman spectra of reduced cytochrome oxidase at several alkaline pH levels are shown in Figure 8. At pH 7.4, with excitation at 406.7 nm, the characteristic vibrations of cytochrome a^{2+} at 1622,

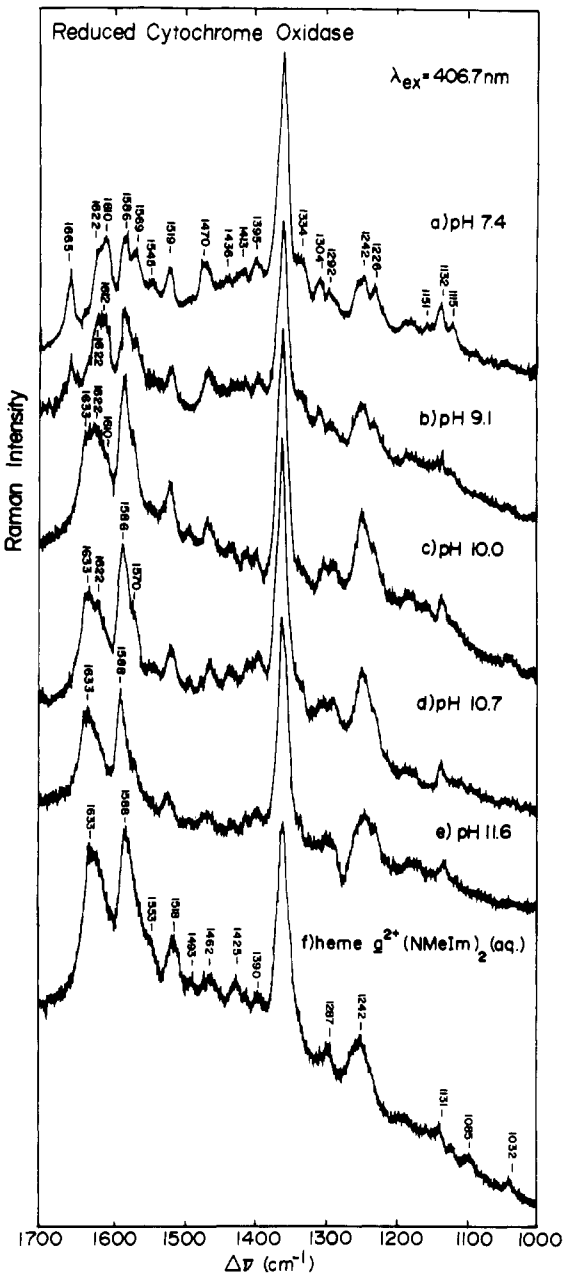

FIGURE 8: Soret excitation resonance Raman spectra of reduced cytochrome oxidase at neutral and alkaline pH (a–e). Enzyme concentration was approximately 40 μM. Sample conditions in (f) are ~50 μM heme *a*, 0.7 M *N*-methylimidazole, 0.07 M CTAB, 0.001 M EDTA, and 0.1 M sodium phosphate, pH 7.4. Instrumental conditions: resolution, 6 cm^{-1}; for (a–e) time constant 2.5 s and scan rate 20 cm^{-1}/min; for (f) time constant 1 s and scan rate 50 cm^{-1}/min.

1610 (~90%), 1586, 1569 (~90%), 1520, and 1358 cm^{-1} and of cytochrome $a_3{}^{2+}$ at 1665, 1610 (~10%), 1569 (~10%), and 1358 cm^{-1} are observed[2] (Table III). The changes that occur as the pH is raised to 9.5 are (a) decreases in intensity at 1665, 1610, and 1115 cm^{-1}, (b) an increase in intensity at 1633 cm^{-1}, and (c) a shift in intensities in the 1220–1250-cm^{-1} region. Since the formyl stretching vibration of cytochrome $a_3{}^{2+}$ at 1665 cm^{-1} is well separated from the other ring vibrations, its

[2] The relative intensities of the characteristic vibrations of ferrous cytochromes *a* and a_3 were obtained by comparison of reduced cytochrome oxidase RR peak heights obtained with 406.7-nm excitation relative to an internal standard ($SO_4{}^{2-}$) with the corresponding peak heights (again with $SO_4{}^{2-}$ as the internal standard) of cytochrome oxidase partially reduced inhibitor complexes (HCN, $HCOO^-$).

Table III: Reduced Cytochrome Oxidase Soret Excitation Heme Chromophore Vibrational Assignments[a]

cytochrome a^{2+}		cytochrome $a_3{}^{2+}$	
$\Delta\bar{\nu}$ (cm^{-1})	assignment	$\Delta\bar{\nu}$ (cm^{-1})	assignment
		1665	ν(C=O)
1622	B_{1g}, ν_{10}	1610	B_{1g}, ν_{10}
1610	H-bonded ν(C=O)		
1586	A_{1g}, ν_2	1575	A_{1g}, ν_2
1569	B_{1g}, ν_{11} or E_u, ν_{38}[b]	1565	B_{1g}, ν_{11} or E_u, ν_{37}[b]
1520	A_{1g}, ν_3	1473	A_{1g}, ν_3
1358	A_{1g}, ν_4	1358	A_{1g}, ν_4

[a] Symmetries and mode numbers from Abe et al. (1978); for further documentation of these assignments, see Salmeen et al. (1978). [b] See Choi et al. (1982).

intensity ratioed to the intensity of ν_4 at 1358 cm^{-1} establishes a titration curve for the pH-dependent changes of cytochrome $a_3{}^{2+}$ (Figure 5). The carbonyl band decreases in intensity with an apparent pK = 9.3, corresponding to the pH range of the initial changes observed by MCD. After complete disappearance of the native cytochrome $a_3{}^{2+}$ formyl vibration (1665-cm^{-1} band) at pH 10, further band changes in the high-frequency region are observed. These consist of an additional decrease in intensity in the 1610-cm^{-1} band with a concomitant increase at 1633 cm^{-1}; the shoulder at 1570 cm^{-1} is no longer strongly observed at pH 11.5. The vibrational spectrum of reduced cytochrome oxidase at pH 11.5 is essentially identical with that of a low-spin ferrous heme *a* model compound in an aqueous environment (Figure 8f), and the band at 1633 cm^{-1} is characteristic of the formyl vibration of heme *a* under these conditions.[3] This second set of vibrational shifts occur in a pH range comparable to the range of cytochrome a^{2+} pH-dependent shifts as determined by visible excitation Raman data. As the pH is increased above 11.5, vibrations characteristic of the Schiff base species are detected (Salmeen et al., 1978).

Discussion

Reduced Cytochrome Oxidase. The original optical/Raman work on cytochrome oxidase at high pH (Salmeen et al., 1978) was somewhat paradoxical in that the major apparent alteration as detected by Raman spectroscopy appeared to occur at cytochrome a_3 while the primary optical shift appeared to involve cytochrome *a* (Lemberg & Pilger, 1964). The present, more detailed study resolves this paradox and shows that for reduced cytochrome oxidase both heme *a* chromophores are gradually modified in structure by alkaline pH. Moreover, these alterations show different pH dependencies which allow us to determine the structural changes responsible for the spectral shifts. The MCD, visible, and Soret excitation Raman data identify three pH-dependent steps: a change in cytochrome a_3 which occurs with a pK ~ 9.3, an alteration of cytochrome *a* with a pK ~ 10.5, and, at pH >11.5, formation of the Schiff base adducts of both chromophores. For the pH range 8.5–10, the optical absorption, MCD, and Soret excitation resonance Raman data suggest a high- to low-spin transition and a solvent environment change at the a_3 site. It has been reported that redox titrations of cytochrome oxidase, monitored by MCD, display unusual behavior above pH 9 (Carithers & Palmer, 1981). This shift in thermodynamic behavior may be a reflection of the structural changes induced in cytochrome a_3 by mildly alkaline conditions.

Cytochrome *a* is affected by somewhat more alkaline conditions. With pK ~ 10.5, its spectral characteristics shift to those of an isolated low-spin heme a^{2+} model compound in an aqueous environment. Soret excitation resonance Raman spectra offer the most insight into the structural changes which occur during this process (Figure 8). One of the major band shifts that occurs in this pH range is the decrease in intensity of the anomalous cytochrome a^{2+} vibration at 1610 cm^{-1} and concomitant increase at 1633 cm^{-1}. From the fact that the 1633-cm^{-1} band arises from a low-spin heme a^{2+} formyl vibration exposed to an aqueous environment (Figure 8f) and from the mirrored shifts in the 1610- and 1633-cm^{-1} vibrations, we assign the 1610-cm^{-1} band observed in the native protein to a perturbed formyl vibration of the cytochrome *a* chromophore. The largest optical absorption changes, from 441 nm, 601 nm to 436 nm, 595 nm, also occur in this pH range, which indicate that the optical properties of cytochrome a^{2+} and the physical state of its formyl group are linked. In view of the significant perturbation of heme optical properties induced by peripheral aldehydes (Gouterman, 1959), such a linkage is not surprising.

The argument above indicates that the absorption red shift of cytochrome *a* in vivo at neutral pH relative to that of its model compounds and the structural alteration of its formyl group are related. This observation, coupled with our earlier results which showed that low-spin heme *a* models accurately reproduce other vibrations of cytochrome *a*, particularly its core-size marker bands (Callahan & Babcock, 1981), provides criteria with which to judge possible models for the structure of the cytochrome *a* site. For example, the presence of nearby polarizing amino acids capable of forming π complexes with the heme *a* system may be expected to alter the spectral properties of cytochrome *a* by analogy with the absorption red shift observed by Mauzerall (1965) for π complexes between aromatic rings and uroporphyrin. However, Shelnutt (1981) has shown that formation of a π complex is accompanied by vibrational frequency changes of several wavenumbers in the high-frequency core-size marker bands. Such frequency shifts are not apparent in the cytochrome *a* Raman spectrum. In addition, metalloporphyrin *a* complexes with π acceptors show only small spectral shifts which are unable to account for the differences between isolated heme *a* and in vivo cytochrome *a* spectral properties (P. M. Callahan, unpublished experiments). A second possible model involves the occurrence of strained or hindered axial ligands to the cytochrome *a* iron which may perturb the optical properties of the chromophore. Carter et al. (1981) have shown that hindered axial ligands shift heme EPR ligand field parameters in a characteristic manner and used their observation to rationalize the liganding in mitochondrial *b* cytochromes. Such an explanation is unlikely for cytochrome *a* owing to our previous EPR results on the chromophore and its models (Babcock et al., 1979a). Moreover, Raman core-size marker bands are perturbed by sterically hindered axial ligands (J. Frentrup, unpublished experiments); such perturbations are not observed in the Raman spectrum of the in vivo chromophore. A third possible means to account for the red-shifted cytochrome *a* absorption spectrum is suggested by studies on rhodopsin and bacteriorhodopsin (Honig et al., 1979; Sheves et al., 1979) and involves the specific arrangement of point charges in the heme *a* binding site of cytochrome *a*. The extension of the external point charge model to tetrapyrrole-based systems has resulted in reports of a range of absorption spectral shifts (Davis et al.,

[3] A thorough characterization of the heme *a* formyl stretching frequency has been carried out (J. Frentrup, P. M. Callahan, and G. Babcock, unpublished experiments).

1981; Eccles & Honig, 1982), but such a model would not be able to account for the altered formyl vibrational frequencies in cytochrome *a* without additional ad hoc assumptions. Point charge effects, however, may be important for the spectroscopy of cytochrome a_3 in isolated cytochrome oxidase and could account for the effects of Ca^{2+} on the absorption properties of various heme *a* species reported by Wikström and coworkers (Saari et al., 1980).

It appears, therefore, that a perturbation to the cytochrome *a* ring system which only indirectly influences the formyl group will not account for the combined optical, Raman, and EPR data; rather, a specific interaction at the carbonyl seems necessary in order to rationalize the spectroscopic results. Structural modifications of the cytochrome *a* formyl group which may explain the observed phenomena include the following: (a) protonated Schiff base formation at the peripheral formyl group, (b) nonplanarity of the position 8 aldehyde with the porphyrin π system, and (c) hydrogen bonding to the peripheral aldehyde. The previously suggested structure of a protonated Schiff base between the cytochrome a^{3+} aldehyde and an ϵ-amino group of a lysine residue of the protein (Ondrias & Babcock, 1980) is not supported by model compound studies (Ward et al., 1983) and can therefore be eliminated as a likely explanation. Nonplanarity of the peripheral aldehyde and porphyrin ring π systems also seems unlikely for two reasons. First, the fact that we observe a high-frequency vibration from a perturbed formyl group indicates that the carbonyl and porphyrin π systems must have some degree of overlap for resonance enhancement to occur. Second, it is difficult to rationalize a red-shifted heme absorption spectrum in both the Soret and α-band regions when the perturbation invoked decreases the extent of conjugation of the porphyrin π system.

In order to effect both a red-shifted absorption spectrum and a decreased formyl stretching frequency, a greater electron-withdrawing capability at the peripheral formyl group is needed. A hydrogen-bonding interaction in which the formyl C=O acts as the proton acceptor provides a reasonable structure within which such effects could occur. The decrease in carbonyl stretching frequency upon hydrogen-bond formation is well-known, and because the visible and Soret absorption bands of heme *a* are $\pi \rightarrow \pi^*$ transitions, an absorption red shift is predicted to result from hydrogen bonding (Pimentel & McClellan, 1960). Moreover, because the hydrogen bond is a specific perturbation to the formyl group, the major porphyrin ring vibrations would not be modified to any great extent, in agreement with our earlier observations. Therefore, we conclude that a hydrogen bond between an amino acid residue and the peripheral aldehyde can explain the spectra of cytochrome *a* and the observed pH-dependent behavior. We have found that there is a general pattern of parallel decreases in frequency of heme *a* absorption maxima and C=O stretching frequencies with increasing hydrogen-bond strength (G. T. Babcock and P. M. Callahan, unpublished experiments). As a result of this, a greater hydrogen-bonding strength than that observed with water as the hydrogen donor is responsible for the spectra of cytochrome *a*. For the ferrous species, (heme a^{2+})$(NMeIm)_2$ in an aqueous environment displays an α-band maximum of 595 nm (16 800 cm^{-1}) and ν(C=O) at 1633 cm^{-1}. Additional decreases in frequency of both these quantities and therefore a greater hydrogen-donating ability is needed to account for the properties of cytochrome a^{2+} in the native enzyme with an α maximum and ν(C=O) at 604 nm (16 550 cm^{-1}) and 1610 cm^{-1}, respectively. We suggest that tyrosine may be the proton-donating group involved in the hydrogen-bond interaction with the cytochrome *a* peripheral aldehyde based on the ability of phenol as a hydrogen donor to low-spin heme *a* model compounds to mimic the cytochrome a^{3+} absorption spectrum (G. T. Babcock and P. M. Callahan, unpublished experiments).

The pH dependence of the hydrogen-bonded form of cytochrome *a* presented above could arise from either a titration of the proton donor group or a disruption of the hydrogen-bonded structure by an alkaline pH induced conformational change of the protein. Since we can monitor only the hydrogen acceptor (C=O) stretching frequency by RRS and not the donor (R–H) stretching frequency, we are unable to distinguish experimentally between these two alternatives. However, the ability to shift the titration curves of the pH-dependent spectral changes to higher pH values by using nondenaturing neutral detergents (Tween-20 and lauryl maltoside; see above) or to lower pH values under more strongly denaturing conditions [$NaDodSO_4$ treatment (Criddle & Bock, 1959), 8 M urea, pH 7.4 (Lemberg & Pilger, 1964), or heat treatment (Person & Zipper, 1964)] suggests that these effects are most likely due to an unfolding of the protein tertiary structure.

By combining this information with our conclusions on the behavior of cytochrome a_3 under alkaline conditions, we can summarize the overall effects of pH on reduced cytochrome oxidase as in the schematic in Figure 9 (left panel). The first pH-dependent step, p$K \sim 9.3$, involves a structural shift at cytochrome a_3, apparently arising from a ligation and solvent environment change. The second pH-dependent step involves cytochrome *a* and is a consequence of the disruption of the hydrogen bond between the position 8 formyl group of the cytochrome *a* ring and the postulated tyrosine residue. This seems to be a result of a protein conformational change caused by the denaturing alkaline conditions. At this pH both cytochromes *a* and a_3 have similar spectral characteristics, that of low-spin ferrous heme *a* in an aqueous environment. Above pH 12, Schiff base formation between the heme *a* aldehydes of both chromophores and ϵ-amino groups of lysine residues is observed (Lemberg, 1964; Takemori & King, 1965). At this point denaturation of the protein may proceed to such an extent that migration of the hemes *a* to other loci on the protein occurs. If this is the case, then the location of lysine residues within the heme pockets of cytochromes *a* and a_3 is not mandatory in our model.

Oxidized Cytochrome Oxidase. As in the reduced enzyme, cytochrome a_3 is first affected by alkaline pH treatment of the oxidized enzyme. The resonance Raman and optical data indicate that a six-coordinate high- to low-spin transition takes place in this chromophore over the pH range 8.5–10. This conclusion rationalizes the decrease in absorbance at 655 nm, which has been attributed to the high-spin cytochrome $a_3{}^{3+}$–$Cu_{a_3}{}^{2+}$ site (Hartzell et al., 1973), and accounts for the shift in the cytochrome $a_3{}^{3+}$ core-size band from 1572 to 1590 cm^{-1}. In a recent study of H_2O_2 binding to cytochrome oxidase, Bickar et al. (1982) reported a change in the optical spectra of the native enzyme and of the peroxide bound form at pH 9.8. These spectral shifts may be a reflection of the spin-state transition induced in cytochrome $a_3{}^{3+}$ by moderately alkaline pH as reported here. No changes in cytochrome a^{3+} in this pH range are observed. At strongly alkaline pH ($\geq$12), both heme chromophores have similar vibrational properties indicative of five-coordinate, high-spin heme a^{3+}. Aggregate or μ-oxo dimer formation at pH 12, as suggested above, is a possible configuration that is consistent with both the EPR and Raman data. Although several structural changes are observed for the heme *a* chromophores in oxidized cytochrome

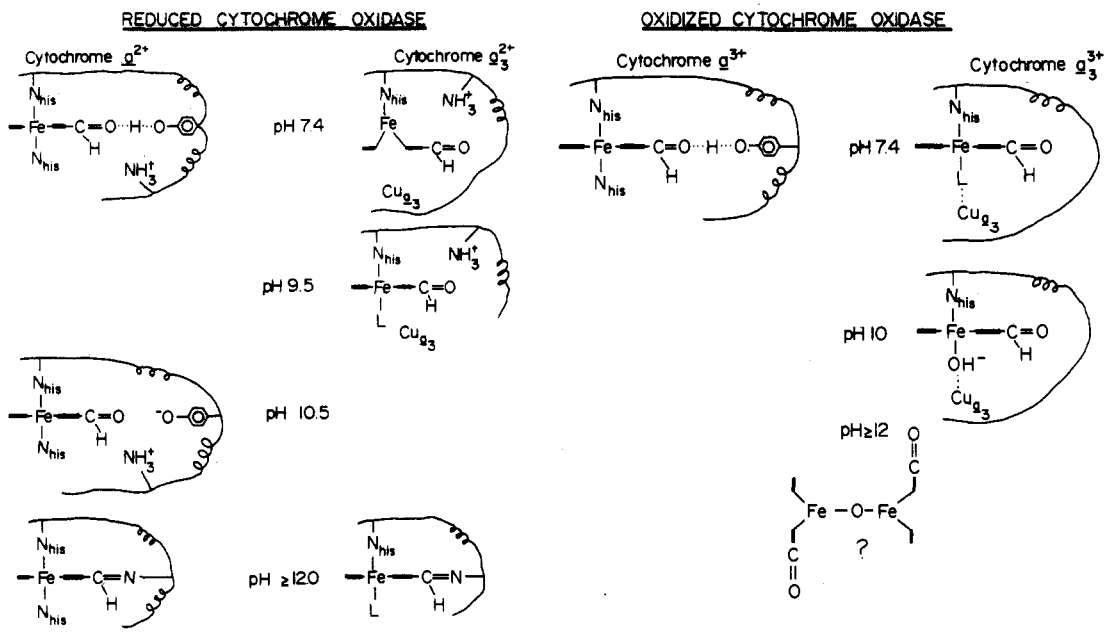

FIGURE 9: Schematic of proposed structural changes of the reduced (left panel) and oxidized (right panel) heme *a* chromophores of cytochrome oxidase at several pH levels. See Discussion for further details.

oxidase under alkaline conditions, the 10-nm red shift in the α-band maximum of cytochrome *a* and its anomalous high-frequency vibration at 1650 cm^{-1} relative to those of low-spin heme *a* model compounds (Table I) are not modified in such a manner as to reveal the nature of these spectral shifts. Noting the fact that (heme a^{3+})$(NMeIm)_2$ reproduces the high-frequency RR vibrations of cytochrome a^{3+} with the exception of the formyl vibration (Babcock et al., 1981) and by reference to the proposed structure of ferrous cytochrome *a* in which a hydrogen-bonded aldehyde structure (Figure 9) lowers the formyl stretching frequency by $\sim$30 cm^{-1}, the 1650-cm^{-1} band of cytochrome a^{3+} is assigned to a perturbed formyl vibration in the oxidized enzyme. The ability of low-spin heme a^{3+} model compounds in the presence of hydrogen donors (e.g., phenol) to mimic the optical and resonance Raman vibrational properties of cytochrome a^{3+} (G. T. Babcock and P. M. Callahan, unpublished experiments) provides additional support for the proposal that the 1650-cm^{-1} band of cytochrome a^{3+} arises from a hydrogen-bonded formyl group. Therefore, we conclude that the hydrogen-bonded formyl configuration is also present in the oxidized enzyme.

A schematic summary of the pH effects on oxidized cytochrome oxidase is shown in Figure 9 (right panel). The native enzyme displays the cytochrome *a* formyl group–tyrosine hydrogen-bonding interaction. As the pH is raised, the optical, Raman and EPR data indicate that cytochrome a_3 undergoes a spin-state transition. In this case, the cytochrome *a* formyl hydrogen-bonded structure remains intact until strongly denaturing conditions are reached, at approximately pH 12, where Raman, optical, and EPR data suggest that the heme *a* chromophores occur as five-coordinate and high-spin hemes, possibly in the configuration of μ-oxo dimers.

The ability to alter the cytochrome *a* formyl–protein interaction at lower pH in the reduced protein than in the oxidized enzyme suggests that the latter is a more compact, stable structure. Further evidence for this protein structural feature lies in the determination of the relative sizes and conformations of different forms of cytochrome oxidase by sedimentation velocity experiments (Cabral & Love, 1972). These results indicate that the reduced enzyme occupies a 3% larger volume than the fully oxidized form of cytochrome oxidase. A further significant difference between the oxidized and reduced forms of the enzyme lies in the shift in the α-band maximum upon reduction. In most heme absorption spectra the position of the α band is unchanged or only slightly modified ($\pm$2 nm) upon redox-state change. The 5-nm red shift in the α band of cytochrome oxidase (essentially the α band of cyt *a*) from 599 to 604 nm upon reduction indicates a stronger interaction of the cytochrome *a* formyl with the H-donor group of the protein in the reduced vs. the oxidized protein (Pimentel & McClellan, 1960; Baum & McClure, 1979). Our initial estimate of the shift in hydrogen-bond energy upon iron redox-state change is roughly 2 kcal/mol. This energy shift and the presumed change in hydrogen-bond length which accompany it provide a pathway by which electron transfer events at the redox active cytochrome *a* iron may be communicated to the surrounding protein matrix. Additional evidence supporting this conclusion and its implications for proton pumping in cytochrome oxidase will be presented elsewhere.

Acknowledgments

We acknowledge the assistance of Robert Ingle in the preparation of beef heart cytochrome oxidase and of Drs. David Ballou, Jules Shafer, and Russell Hille at the University of Michigan and Steve Worland and Ken Sauer of the University of California, Berkeley, for the use of their optical and MCD spectrophotometers.

Registry No. 1, 57560-10-8; cytochrome oxidase, 9001-16-5; cytochrome *a*, 9035-34-1; cytochrome a_3, 72841-18-0.

References

Abe, M., Kitagawa, T., & Kyogoku, Y. (1978) *J. Chem. Phys. 69*, 4526–4534.

Alben, J. O., Moh, P. P., Fiamingo, F. G., & Altschuld, R. A. (1981) *Proc. Natl. Acad. Sci. U.S.A. 78*, 234–237.

Artzatbanov, V. Y., Konstantinov, A. A., & Skulachev, V. P. (1978) *FEBS Lett. 87*, 180–185.

Aton, B., Doukas, A.G., Callender, R. H., Becher, B., & Ebrey, T. G. (1977) *Biochemistry 16*, 2995–2999.

Azzi, A. (1981) *Biochim. Biophys. Acta 594*, 231–252.

Babcock, G. T. (1982) in *Inorganic Reactions and Methods*, Verlag Chemie (in press).

Babcock, G. T., & Salmeen, I. (1979) *Biochemistry 18*, 2493–2498.
Babcock, G. T., Vickery, L. E., & Palmer, G. (1976) *J. Biol. Chem. 251* 7907–7919.
Babcock, G. T., Vickery, L. E., & Palmer, G. (1978) *J. Biol. Chem. 253*, 2400–2411.
Babcock, G. T., Van Steelandt, J., Palmer, G., Vickery, L. E., & Salmeen, I. (1979a) in *Developments in Biochemistry, Volume 5: Cytochrome Oxidase* (King, T. E., Orii, Y., Chance, B., & Okunuki, K., Eds.) pp 105–115, Elsevier, Amsterdam.
Babcock, G. T., Ondrias, M. R., Gobeli, D. A., Van Steelandt, J., & Leroi, G. E. (1979b) *FEBS Lett. 108*, 147–151.
Babcock, G. T., Callahan, P. M., Ondrias, M. R., & Salmeen, I. (1981) *Biochemistry 20*, 959–966.
Baum, J. C., & McClure, D. S. (1979) *J. Am. Chem. Soc. 101*, 2340–2343.
Bickar, D., Bonaventura, J., & Bonaventura, C. (1982) *Biochemistry 21*, 2661–2666.
Blumberg, W. E., & Peisach, J. (1979) *Dev. Biochem. 5*, 153–159.
Bocian, D. F., Lemley, A. T., Peterson, N. O., Brudvig, G. W., & Chan, S. I. (1979) *Biochemistry 18*, 4396–4402.
Brudvig, G. W., Stevens, T. H., Morse, R. H., & Chan, S. I. (1981) *Biochemistry 20*, 3912–3921.
Cabral, F., & Love, B. (1972) *Biochim. Biophys. Acta 238*, 181–186.
Callahan, P. M., & Babcock, G. T. (1981) *Biochemistry 20*, 952–958.
Callahan, P. M., & Babcock, G. T. (1982) *Proc. Int. Conf. Raman Spectrosc., 8th*, 739–740.
Carithers, R. P., & Palmer, G. (1981) *J. Biol. Chem. 256*, 7967–7976.
Carter, K., Tsai, A., & Palmer, G. (1981) *FEBS Lett. 132*, 243–246.
Caughey, W. S., Smythe, G. A., O'Keeffe, D. H., Maskasky, J. E., & Smith, M. L. (1975) *J. Biol. Chem. 250*, 7602–7622.
Chan, S. H. P., Love, B., & Stotz, E. (1970) *J. Biol. Chem. 245*, 6669–6674.
Choi, S., Spiro, T. G., Langry, K. C., Smith, K. N., Budd, D. L., & LaMar, G. N. (1982) *J. Am. Chem. Soc. 104*, 4345–4351.
Criddle, R. S., & Bock, R. M. (1959) *Biochim. Biophys. Res. Commun. 1*, 138–142.
Davis, R. C., Ditson, S. L., Fentiman, A. F., & Pearlstein, R. M. (1981) *J. Amer. Chem. Soc. 103*, 6823–6826.
Eccles, J., & Honig, B. (1982) *Biophys. J. 37*, 228a.
Gouterman, M. (1959) *J. Chem. Phys. 30*, 1139–1161.
Halaka, F. G. (1981) Ph.D. Thesis, Michigan State University.
Halaka, F. G., Babcock, G. T., & Dye, J. L. (1981) *J. Biol. Chem. 256*, 1084–1087.
Hartzell, C. R., & Beinert, H. (1974) *Biochim. Biophys. Acta 368*, 318–338.
Hartzell, C. R., Hansen, R. E., & Beinert, H. (1973) *Proc. Natl. Acad. Sci. U.S.A. 70*, 2477–2481.
Honig, B., Dinur, U., Nakanishi, K., Balogh-Nair, V., Gawinowicz, M. A., Arnaboldi, M., & Motto, M. G. (1979) *J. Am. Chem. Soc. 101*, 7084–7086.
Lemberg, R. (1962) *Nature (London) 193*, 373–374.
Lemberg, R. (1964) *Proc. R. Soc. London, Ser. B 159*, 429–435.
Lemberg, R., & Pilger, T. B. G. (1964) *Proc. R. Soc. London, Ser. B 159*, 436–448.
Malmström, B. G. (1974) *Q. Rev. Biophys. 6*, 389–431.
Malmström, B. G. (1979) *Biochim. Biophys. Acta 549*, 281–303.
Marcus, M. A., Lemley, A. T., & Lewis, A. (1979) *J. Raman Spectrosc. 8*, 22–25.
Mathies, R., Freedman, T. B. & Stryer, L. (1977) *J. Mol. Biol. 109*, 367–372.
Mauzerall, D. (1965) *Biochemistry 4*, 1801–1810.
Ondrias, M. R., & Babcock, G. T. (1980) *Biochem. Biophys. Res. Commun. 93*, 29–35.
Person, P., & Zipper, H. (1964) *Biochim. Biophys. Acta 92*, 605–607.
Pimentel, G. C., & McClellan, A. L. (1960) *The Hydrogen Bond*, pp 157–164, W. H. Freeman, San Francisco.
Saari, H., Pentillä, T., & Wikström, M. (1980) *J. Bioenerg. Biomembr. 12*, 325–338.
Salmeen, I., Rimai, L., & Babcock, G. T. (1978) *Biochemistry 17*, 800–806.
Scott, R. A., & Gray, H. B. (1980) *J. Am. Chem. Soc. 102*, 3219–3224.
Shelnutt, J. A. (1981) *J. Am. Chem. Soc. 103*, 4275–4277.
Sheves, M., Nakanishi, K., & Honig, B. (1979) *J. Am. Chem. Soc. 101*, 7086–7088.
Solioz, M., Carafoli, E., & Ludwig, B. (1982) *J. Biol. Chem. 257*, 1579–1582.
Spaulding, L. D., Chang, C. C., Yu, N.-T., & Felton, R. H. (1975) *J. Am. Chem. Soc. 97*, 2517–2525.
Spiro, T. G., Stong, J. D., & Stein, P. (1979) *J. Am. Chem. Soc. 101*, 2648–2655.
Sutherland, J. C., Vickery, L. E., & Klein, M. P. (1974) *Rev. Sci. Instrum. 45*, 1089–1094.
Takemori, S., & King, T. E. (1965) *J. Biol. Chem. 240*, 504–513.
Tsubaki, M., Nagai, K., & Kitagawa, T. (1980) *Biochemistry 19*, 379–385.
Tweedle, M. F., Wilson, L. J., García-Iñiguez, L., Babcock, G. T., & Palmer, G. (1978) *J. Biol. Chem. 253*, 8065–8071.
Vanneste, W. H. (1966) *Biochemistry 5*, 838–848.
Van Steelandt-Frentrup, J., Salmeen, I., & Babcock, G. T. (1981) *J. Am. Chem. Soc. 103*, 5981–5982.
Van Verseveld, H. W., Krab, K., & Stouthamer, A. H. (1981) *Biochim. Biophys. Acta 635*, 525–534.
Ward, B., Callahan, P. M., Young, R., Babcock, G. T., & Chang, C. K. (1983) *J. Am. Chem. Soc.* (in press).
Wever, R., Van Ark, G., & Van Gelder, B. F. (1977) *FEBS Lett. 84*, 388–390.
Wikström, M. K. F. (1977) *Nature (London) 266*, 271–273.
Wikström, M. K. F., & Saari, H. T. (1977) *Biochim. Biophys. Acta 462*, 347–361.
Wikström, M., & Krab, K. (1979) *Biochim. Biophys. Acta 549*, 177–222.
Wikström, M. K. F., Harmon, H. J., Ingledew, W. J., & Chance, B. (1976) *FEBS Lett. 65*, 259–277.
Wikström, M., Krab, K., & Saraste, M. (1981) *Cytochrome Oxidase: A Synthesis*, Academic Press, London.
Wilson, M. T., Colosimo, A., Brunori, M., & Antonini, E. (1978) *Frontiers of Biological Energetics* (Dutton, P. L., et al., Eds.) pp 843–850, Academic Press, New York.
Woodruff, W. H., Dallinger, R. F., Antalis, T. M., & Palmer, G. (1981) *Biochemistry 20*, 1332–1338.